Vladimir M. SHATOKHIN[1], Vladimir N. SOBOL[1], Waldemar WÓJCIK[2], Gali DUSKAZAEV[3], Daniyar JARYKBASSOV[3]

Kharkiv National University of Civil Engineering and Architecture (1),
Lublin University of Technology (2), Kazakh Academy of Transport & Communication (3)

Dynamical processes simulation of unbalanced vibration devices with eccentric rotor and induction electric drive

Abstract. A complex mathematical model of dynamic processes in vibration device on elastic supports with eccentric self-centering unbalanced rotor and induction motor is given. A working chamber of induction motor does a plane motion. The dynamic feature of the electric motor is chosen for descriptions of device starting and a load oscillating character at steady-state modes of the device. Such model allows: to choose the electric motor of necessary power, to study influence of unbalances, to study influence of the rotor eccentricity and other drive parameters at the device starting, movement of characteristic points of its chamber, loads on bearings and the foundation. It has been established that a rational choice of eccentricity lead to the rotor vibrations reduce – realization of the self-centering effect. A visual method for geometric interpretation of the dynamic processes development at the device starting is proposed. Calculations results for the device with specific size are presented. The completed researches are perspective for solve problems of rational parameters choice for the considered class of mechanisms.

Streszczenie. I Przedstawiono model matematyczny procesów dynamicznych w urządzeniu wibracyjnym na elastycznych wspornikach z ekscentrycznym, samocentrującym niezrównoważonym wirnikiem i silnikiem indukcyjnym. Część robocza silnika indukcyjnego wykonuje ruch płaski. Dynamiczna cecha silnika elektrycznego jest wybierana dla opisów urządzenia rozruchowego i charakteru oscylującego obciążenia w trybach stanu ustalonego urządzenia. Model taki pozwala: wybrać silnik elektryczny o wymaganej mocy, zbadać wpływ asymetrii, zbadać wpływ ekscentryczności wirnika i innych parametrów napędu przy uruchomieniu urządzenia, ruch charakterystycznych punktów jego komory, obciążenia na łożyskach i fundamencie. Ustalono, że odpowiedni wybór ekscentryczności prowadzi do zmniejszenia wibracji wirnika - realizacja efektu samocentrującego. Zaproponowano wizualną metodę geometrycznej interpretacji dynamicznego rozwoju procesów przy uruchamianiu urządzenia. Przedstawiono wyniki obliczeń dla urządzenia o określonej wielkości. (Symulacja procesów dynamicznych niezrównoważonych urządzeń wibracyjnych z ekscentrycznym wirnikiem i indukcyjnym napędem elektrycznym).

Keywords: dynamical process, vibration device, unbalance, eccentric rotor, induction motor.
Słowa kluczowe: proces dynamiczny, urządzenie wibracyjne, niewyważenie, wirnik mimośrodowy, silnik indukcyjny.

Introduction

A using of vibration technologies allows intensify production processes, improve the work quality, create materials with new properties, reduce the material and energy intensities of equipments [1]. Vibration machines on elastic supports with an eccentric rotor, unbalances and an induction electric drive have several advantages. The constructions of such mechanisms are simple, but their motion parameters can be determined only by dynamic analysis, since the devices perform oscillations [1, 2].
Additional difficulties are caused with correct description of the dynamic feature of an induction motor (IM) at transient modes and a load with oscillating character [3].
Investigations of dynamical processes simulation, parameters choice, predictions of technological qualities for devices are very significant and urgency.

At present, mathematical models of vibration devices are not sufficiently developed. In the papers [4, 5], the motion equations of the simplest mechanism model are obtained at steady-state operating modes and under the assumption that a working chamber performs translational motion. However, in most cases the translational motion conditions are not met. In addition, frequent starts and stops of devices are the characteristic modes of its operations, so the calculations of transient processes are very relevant. The cheap and easy-to-use IM generates additional difficulties associated with the description of its dynamic features at transient modes and a load with oscillating character. The using of linearized static characteristics [6], or linearized differential equations [7], which approximately describe electromagnetic transient processes in electric motors, leads to a significant overestimating of the calculated torque of IM compared with the experimental one [3].

An absence of reliable mathematical models makes it difficult: a choice of motors that provide start-up of devices; a parameters determining of the working chamber oscillations, which are affected on a technological process; rational choice of design parameters that reduce a vibrations transmission to the foundation, a load on bearings, the material and energy intensities of devices, etc. The research objective is the creation of a complex mathematical model of dynamic processes in a vibration device on elastic supports with an eccentric self-centering unbalanced rotor and an induction motor drive whose working chamber does a plane motion. The following problems must be solved: to create differential equations of dynamic processes for the device mechanical part; to determine the motor dynamic feature, which adequately describes the process of the device starting and a load with oscillating character at steady-state modes of the device; to propose the converting method for consistent system of differential equations to a convenient form for numerical integration; to give a visual method for geometric interpretation of the dynamic processes development at the device starting.

Computational studies with the help of the developed model are carried out to found the influences on unbalances, the rotor eccentricity on the device launching process, the characteristic point's movement of its chamber, loads on bearings and the foundation, reducing of the rotor vibrations.

Mathematical model of dynamic processes of vibration device

In Fig. 1 the device scheme have been shown. Working chamber 3 of device is mounted on four vertical spring's 6, rigidly connected with the foundation 7. On two bearings rigidly connected to the chamber a crank of eccentric (e – eccentricity) shaft (rotor, 4) is fixed, on which imbalances 5 are fixed. The rotor is connected by a flexible shaft (durite, 2) to the motor shaft.

Motion equations of the device can be written in the form of Lagrange's equations of the second kind. The

device scheme in the current position is shown in Fig. 2. Generalized coordinates of the mechanical system: the rotation angles of the motor rotor and the device rotor, ψ and φ respectively; Cartesian coordinates x and y, which are determine the mass center position of the working chamber (point C) relative to the basic (fixed) coordinate system Oxy; rotation angle of the working chamber ϑ. In an equilibrium state points C and O are coincide ($Cx''y''$ – translationally moving coordinate system; $Cx'y'$ – moving coordinate system which rigidly connected with the body).
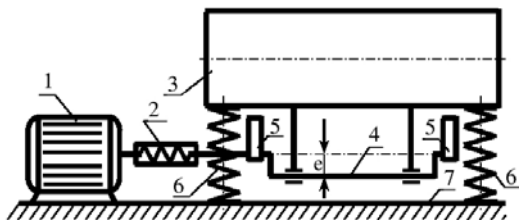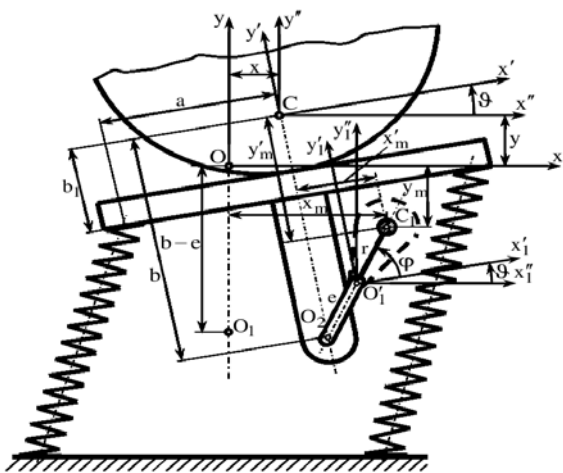

Fig.1. Scheme of vibration device

Fig.2. Design scheme of vibration device

In further the following notation is needed: x'_m, y'_m and x_m, y_m – coordinates of the rotor mass centre (point C_1) respectively in moving and main coordinate system; r – distance from the rotor axis (point O'_1) to the rotor mass centre; b – distance from mass centre of working chamber to bearings axis; a, b_1 – parameters for position determinations of fixation points of springs upper ends; spring $O_1O'_1$ (is not shown on the figure) performs elastic properties simulations of a flexible shaft (motor axis passes through the point O_1; shaft axis – through the point O'_1; eccentric axis – through the point O_2); H_0 – length of the deformed spring; k_x, k_y, k_ϑ – stiffness of the springs on the shear, tensile-compression and rotation respectively; $\Delta_0 = (M+m)g/4k_y$ – spring initial deformation; $H = H_0 - \Delta_0$ – length of the statically deformed spring; k – stiffness of the flexible shaft on torsion; k_r – bending stiffness of the flexible shaft; g – gravity acceleration.

The equation for the total kinetic energy of system bodies (working chamber T_1, rotor T_2, motor rotor T_3) can be written in the follow form:

$$
\begin{aligned}
T &= T_1 + T_2 + T_3 = \frac{1}{2}(M+m)\dot{x}^2 + \frac{1}{2}(M+m)\dot{y}^2 + \\
&+ \frac{1}{2}\left\{ J + m\left[(e+r)^2 + b^2 - 2(e+r)b\,sin\varphi\right] + I \right\}\dot{\vartheta}^2 + \\
&+ \frac{1}{2}\left[m(e+r)^2 + I\right]\dot{\varphi}^2 + \frac{1}{2}J_e\dot{\psi}^2 - m\left[(e+r)sin\varphi - b\right]\dot{x}\dot{\vartheta} + \\
&+ m(e+r)cos\varphi\,\dot{y}\dot{\vartheta} - m(e+r)sin\varphi\,\dot{x}\dot{\varphi} + m(e+r)cos\varphi\,\dot{y}\dot{\varphi} + \\
&+ \left\{I + m(e+r)\left[(e+r) - b\,sin\varphi\right]\right\}\dot{\vartheta}\dot{\varphi}
\end{aligned}
\tag{1}
$$

where M – total mass of the working chamber and processed material; m – mass of all rotor rotating parts (including the eccentric shaft mass m_v, its diameter d_v, and mass of two unbalances $2m_d$; distance from the mass center of unbalances to the shaft axis r_d); J – axial inertia moment of the working chamber, axis pass through the mass center C; I – inertia moment of the rotor, axis pass through the mass center C_1; J_e – inertia moment of the motor. It was assumed in the equation (1) that coordinates changes x, y, ϑ near the stable equilibrium It was assumed in the equation (1) that coordinate changes x, y, ϑ near positions of a stable equilibrium $x = y = \vartheta = 0$ are small. Therefore it can be written, that $sin(\varphi + \vartheta) \approx sin\varphi$, $cos(\varphi + \vartheta) \approx cos\varphi$.

The system potential energy is a combination of the position energy and the deformation energy of elastic connections.

The potential energy of gravity can be written:

$$
\Pi_1 = (M+m)gy + mg\left[b(1 - cos\,\vartheta) - (e+r)\left(1 - sin(\varphi + \vartheta)\right)\right]
\tag{2}
$$

The potential energy of tension-compression for four springs can be presented in the form:

$$
\begin{aligned}
\Pi_2 = 2k_y\Big\{ &x^2 + (H+y)^2 + \\
&+ 2\left[a^2 + b_1^2 + b_1(H+y)\right](1 - cos\,\vartheta) + 2x \cdot b_1\,sin\,\vartheta - \\
&- \left[\sqrt{h_1(x,y,\vartheta)} + \sqrt{h_2(x,y,\vartheta)}\right]H_0 + H_0^2 - \Delta_0^2 \Big\}
\end{aligned}
\tag{3}
$$

where:

$$
\begin{aligned}
h_1(x,y,\vartheta) &= x^2 + (H+y)^2 + \\
&+ 2\left[a^2 + b_1^2 + x \cdot a + b_1(H+y)\right](1 - cos\,\vartheta) + ; \\
&+ 2\left[x \cdot b_1 - a(H+y)\right]sin\,\vartheta
\end{aligned}
$$

$$
\begin{aligned}
h_2(x,y,\vartheta) &= x^2 + (H+y)^2 + \\
&+ 2\left[a^2 + b_1^2 - x \cdot a + b_1(H+y)\right](1 - cos\,\vartheta) + + \\
&\quad 2\left[x \cdot b_1 + a(H+y)\right]sin\,\vartheta
\end{aligned}
$$

The shear potential energy of four springs:

$$
\Pi_3 = 2k_x\left[(x + b_1\,sin\,\vartheta)^2 + a^2(1 - cos\,\vartheta)^2\right].
\tag{4}
$$

The potential energy of rotation for four springs:

$$
\Pi_4 = 2k_\vartheta\,\vartheta^2.
\tag{5}
$$

The potential energy of bending for the flexible shaft:

$$
\begin{aligned}
\Pi_5 = \frac{k_r}{2}\Big\{ &x^2 + y^2 + 2\Big[x \cdot b\,sin\,\vartheta + x \cdot e\,cos(\varphi + \vartheta) - \\
&- y(e-b) - y \cdot b\,cos\,\vartheta + y \cdot e\,sin(\varphi + \vartheta) + b(e-b)cos\,\vartheta - \\
&- e(e-b)sin(\varphi + \vartheta) - eb\,sin\varphi + e^2 + b^2 - e \cdot b \Big] \Big\}
\end{aligned}
\tag{6}
$$

The potential energy of torsion for the flexible elastic shaft:

(7) $\Pi_6 = \dfrac{1}{2}k(\varphi-\psi)^2$.

The total potential energy of the system can be represented as

(8) $\Pi = \sum\limits_{k=1}^{6}\Pi_k$,

in Maclaurin series near the static equilibrium position. Taking to account summands not higher than second order of smallness with respect to variables x, y, ϑ, it can be obtained the follow expressions for generalized forces:

(9)
$$Q_x = -\frac{\partial\Pi}{\partial x} = -\left[4\left(k_x - \frac{\Delta_0}{H}k_y\right)+k_r\right]x -$$
$$-\left[4b_1\left(k_x - \frac{\Delta_0}{H}k_y\right)+k_r(b-e\,sin\,\varphi)\right]\vartheta - k_r e\,cos\,\varphi \; ;$$

(10)
$$Q_y = -\frac{\partial\Pi}{\partial y} = -\left(4k_y + k_r\right)y -$$
$$-k_r\cdot e\,cos\,\varphi\vartheta + k_r\cdot e(1-sin\,\varphi) \; ;$$

(11).
$$Q_\vartheta = -\frac{\partial\Pi}{\partial\vartheta} = -\left[4b_1\left(k_x - \frac{\Delta_0}{H}k_y\right)+k_r(b-e\,sin\,\varphi)\right]x -$$
$$-k_r e\,cos\,\varphi y - \left\{m\cdot g\cdot b + 4k_y\left[a^2 - b_1(b_1+H)\frac{\Delta_0}{H}\right]+\right.$$
$$\left. +4k_\vartheta - k_r(e-b)b + 4k_x b_1^2 - \left[m\cdot g(e+r)-k_r(e-b)e\right]sin\,\varphi\right\}\vartheta -$$
$$-\left[m\cdot g(e+r)-k_r\cdot e(e-b)\right]cos\,\varphi$$

(12)
$$Q_\varphi = -\frac{\partial\Pi}{\partial\varphi} = k_r ex\,sin\,\varphi - k_r ey\,cos\,\varphi +$$
$$\left[mg(e+r)-k_r e(e-b)\right]\vartheta\,sin\,\varphi -$$
$$-\left[mg(e+r)-k_r e^2\right]cos\,\varphi - k(\varphi-\psi) \; ;$$

(13) $Q_\psi = -\dfrac{\partial\Pi}{\partial\psi} = k(\varphi-\psi)$.

A correct mathematical description of the resistance forces is a difficult problem. However, influence of the resistance forces can be neglected, when we study transient modes and the forced oscillations above resonance typical for considered devices. For refined calculations it must be taking to account following things. For mentioned modes, the integral effect of resistance forces action is so important. So for a simpler description, the generalized resistance forces were assumed to be proportional to the corresponding generalized velocities $\dot x$, y, ϑ, i.e. in the form $Q_x^* = -\beta_x \dot x$, $Q_y^* = -\beta_y \dot y$, $Q_\vartheta^* = -\beta_\vartheta \dot\vartheta$. Damping of the section of the flexible shaft - is proportional to difference between generalized velocities in the form $\beta_\gamma(\dot\varphi-\dot\psi)$. Resistance torque M_d of the vibration device rotor is constant.

Dynamic feature of induction motor.

A rotational torque M_D is acted to the motor rotor, which is determined by the dynamic feature of IM. Its descriptions, as mentioned above, for the considered devices and operating modes are a difficult problem. The analysis allowed to give a preference to the approach proposed in [8, 13, 14].

For the corresponding differential equation it has been used the assumption, that the active stator resistance can be neglected in comparing with the active rotor resistance. It has been shown by researches that differences between the calculated and experimental torques in this case is no more 10%. The dynamic feature can be written in the form:

(14) $T_D^2\xi\ddot M_D + T_D\xi\left(2-\dfrac{T_D}{s}\dot s\right)\dot M_D + \left(1-\dfrac{T_D\xi}{s}\dot s\right)M_D = 2\xi M_k\beta$,

where M_D – motor torque at the transient process; M_k – critical torque of the motor; $\xi = \dfrac{1}{1+\beta^2}$; $\beta = \dfrac{\omega_0-\psi}{\omega_0}$ – relative sliding; ω_0 – angular speed of an ideal stroke; ψ – angular speed of the motor at the transient process; $s = \omega_0 - \psi$ – current sliding; $T_D = \dfrac{1}{\omega_c s_k}$ – electromagnetic time constant; $\omega_c = 50\cdot2\pi$ – angular frequency of the mains voltage; $s_k = \left(s_n + \sqrt{s_n\dfrac{\mu_m-1}{\mu_i-1}}\right)\Big/\left(1+\sqrt{s_n\dfrac{\mu_m-1}{\mu_i-1}}\right)$ – critical sliding [9]; $s_n = \dfrac{\omega_0-\omega_n}{\omega_0}$ – nominal sliding; ω_n – nominal angular speed; $\mu_m = \dfrac{M_k}{M_n}$; $\mu_u = \dfrac{M_s}{M_n}$; $\mu_i = \dfrac{\mu_m}{\mu_u}$; M_n , M_s – nominal and starting torque of the motor respectively.

Motion differential equation of vibration device.

For compactly representations of motion equations let's consider following designations:

$\alpha_1 = M+m$, $\alpha_2 = m(e+r)$, $\alpha_3 = m(e+r)^2 + I$, $\alpha_4 = g\cdot\alpha_2$,

$\alpha_5 = b\cdot\alpha_2$, $\alpha_6 = m\cdot b$, $\delta = \Delta_0/H$, $\alpha_7 = 4(k_x - \delta\cdot k_y)$,

$\alpha_8 = \alpha_7\cdot b_1$, $\alpha_9 = 4k_y$, $\alpha_{10} = J + \alpha_3 + m\cdot b^2$, $\alpha_{11} = 2\alpha_5$,

$\alpha_{12} = m\cdot g\cdot b + 4k_y\left[a^2 - b_1(b_1+H)\delta\right]+4k_\vartheta + 4k_x\cdot b_1^2$,

$\alpha_{13} = k_r\cdot e$, $\alpha_{14} = \alpha_{13}\cdot e$, $\alpha_{15} = \alpha_4 - \alpha_{14}$, $\alpha_{16} = \alpha_{13}(e-b)$,

$\alpha_{17} = \alpha_4 - \alpha_{16}$, $\alpha_{18} = \alpha_7 + k_r$, $\alpha_{19} = k_r\cdot b$, $\alpha_{20} = \alpha_8 + \alpha_{19}$,

$\alpha_{21} = \alpha_9 + k_r$, $\alpha_{22} = k_r(e-b)b$, $\alpha_{23} = \alpha_{12} - \alpha_{22}$.

After standard operations performing for formation of Lagrange equations of the second kind and taking into account the dynamic feature of IM, the following system of differential equations can be obtained:

(15)
$$\begin{cases} \ddot\psi = f_\psi, \\ \alpha_3\cdot\ddot\varphi - \alpha_2\,sin\,\varphi\cdot\ddot x + \alpha_2\,cos\,\varphi\cdot\ddot y + \\ \quad +(\alpha_3 - \alpha_5\,sin\,\varphi)\ddot\vartheta = f_\varphi, \\ -\alpha_2\,sin\,\varphi\cdot\ddot\varphi + \alpha_1\cdot\ddot x + (\alpha_6 - \alpha_2\,sin\,\varphi)\ddot\vartheta = f_x, \\ \alpha_2\,cos\,\varphi\cdot\ddot\varphi + \alpha_1\cdot\ddot y + \alpha_2\,cos\,\varphi\cdot\ddot\vartheta = f_y, \\ (\alpha_3 - \alpha_5\,sin\,\varphi)\ddot\varphi + (\alpha_6 - \alpha_2\,sin\,\varphi)\ddot x + \alpha_2\,cos\,\varphi\cdot\ddot y + \\ \quad +(\alpha_{10} - \alpha_{11}\,sin\,\varphi)\ddot\vartheta = f_\vartheta, \\ \dot M_D = f_{M_D}, \end{cases}$$

where $f_\psi = \dfrac{k}{J_e}(\varphi-\psi) + \dfrac{\beta_\gamma}{J_e}(\dot\varphi-\dot\psi) + \dfrac{M_D}{J_e}$;

$$f_\varphi = \alpha_{13}\,sin\,\varphi\cdot\dot x - \alpha_{13}\,cos\,\varphi\cdot\dot y -$$
$$\alpha_2\left[(\dot x + b\dot\vartheta)cos\,\varphi + \dot y\cdot sin\,\varphi\right]\dot\vartheta -$$
$$-\alpha_{15}\,cos\,\varphi + \alpha_{17}\,sin\,\varphi\vartheta - k(\varphi-\psi) - \beta_\gamma(\dot\varphi-\dot\psi) - M_d \; ;$$

$$f_x = \alpha_2\,cos\,\varphi\cdot(\dot\varphi + \dot\vartheta)\dot\varphi - \alpha_{18}\cdot x - (\alpha_{20} - \alpha_{13}\,sin\,\varphi)\vartheta -$$
$$-\alpha_{13}\,cos\,\varphi - \beta_x\cdot\dot x \; ;$$

$$f_y = \alpha_2 \sin\varphi \cdot (\dot\varphi + \dot\vartheta) \, \dot\varphi - \alpha_{21} y -$$
$$- \alpha_{13} \cos\varphi \cdot \ddot\vartheta + \alpha_{13}(1 - \sin\varphi) - \beta_y \dot y \; ;$$
$$f_\vartheta = \alpha_5 \cos\varphi \cdot (\dot\varphi + 2\dot\vartheta) \, \dot\varphi + \alpha_2 (\dot x \cos\varphi + \dot y \sin\varphi) \, \dot\varphi -$$
$$- (\alpha_{20} - \alpha_{13} \sin\varphi) x - \alpha_{13} \cos\varphi \cdot y - (\alpha_{23} - \alpha_{17} \sin\varphi) \vartheta -$$
$$- \alpha_{17} \cos\varphi - \beta_\vartheta \dot\vartheta$$

$$f_{M_D} = -\omega_c s_k \left\{ 2 + \frac{\left[k(\dot\varphi - \dot\psi) + \beta_\gamma (\ddot\varphi - \ddot\psi) + \dot M_D \right]}{\omega_c s_k (\omega_0 - \dot\psi) J_e} \right\} \dot M_D -$$
$$- \left\{ \omega_c^2 s_k^2 \left[1 + \frac{(\omega_0 - \dot\psi)^2}{\omega_0^2} \right] + \right.$$
$$\left. + \omega_c s_k \frac{\left[k(\dot\varphi - \dot\psi) + \beta_\gamma (\ddot\varphi - \ddot\psi) + \dot M_D \right]}{(\omega_0 - \dot\psi) J_e} \right\} M_D +$$
$$+ 2 M_k \omega_c^2 s_k^2 \frac{(\omega_0 - \dot\psi)}{\omega_0} .$$

Last equation of the system (15) is the expression (14) solved for $\ddot M_D$ and taking to account the above formulas for the parameters. In the derivative by time of the current sliding $\dot s$, the second derivative of the rotation angle of the motor rotor $\ddot\psi$ is replaced by the corresponding expression from the first equation of the stated above system. Thus, the first and last equations of this system are solved for the second derivative of one of the variables. However, integration of the equations system (15) directly by using of widely algorithms for numerical integration is impossible, since the equations 2÷5 of this system are not solved for the second derivative for the each generalized coordinates φ, x, y, ϑ. If the matrix formed from the coefficients of the second derivatives of the specified coordinates on the left side of these equations,

$$(16) \; \mathbf{A} = \begin{bmatrix} \alpha_3 & -\alpha_2 \sin\varphi & \alpha_2 \cos\varphi & \alpha_3 - \alpha_5 \sin\varphi \\ -\alpha_2 \sin\varphi & \alpha_1 & 0 & \alpha_6 - \alpha_2 \sin\varphi \\ \alpha_2 \cos\varphi & 0 & \alpha_1 & \alpha_2 \cos\varphi \\ \alpha_3 - \alpha_5 \sin\varphi & \alpha_6 - \alpha_2 \sin\varphi & \alpha_2 \cos\varphi & \alpha_{10} - \alpha_{11} \sin\varphi \end{bmatrix}$$

had constant elements, then forming of the inverse matrix $\mathbf{A}^{-1}$ and, consequently, equations representing in a convenient form for numerical integration can be a trivial problem. Since the matrix elements are variable, a finding of its inverse matrix is difficult problem, even for the matrix with dimension 4×4. At present time a difficulties in this case can be significantly decreased, but results reliability can be increased by using mathematical packages that include symbolic mathematics. In the paper for such case the Mathcad package has been used [10, 15, 16]. Now the four equations solved for the second derivatives can be presented in the form:

$(17) \; \mathbf{z} = \mathbf{A}^{-1} \mathbf{f}$,

where $\mathbf{z} = [\ddot\varphi, \ddot x, \ddot y, \ddot\vartheta]^T$, $\mathbf{f} = [f_\varphi, f_x, f_y, f_\vartheta]^T$.

The matrix $\mathbf{A}^{-1}$ is not shown here due to it cumbersomeness.

Choice of the induction motor and parameters for the unbalanced vibration device with an eccentric rotor

The developed mathematical model is used to study dynamic processes in the vibration device with the volume $0,2 \, \text{m}^3$ and follow parameters:

$M = 300 \, \text{kg}$, $\quad m_v = 20.71 \, \text{kg}$, $\quad m_d = 7.69 \, \text{kg}$, $\quad m = 36.09 \, \text{kg}$,
$e = 0.0025 \, \text{m}$, $\quad r_d = 0.0785 \, \text{m}$, $r = 0.03345 \, \text{m}$, $\quad d_v = 0.065 \, \text{m}$,
$I = 0.06539 \, \text{kg} \cdot \text{m}^2$, $J = 9.375 \, \text{kg} \cdot \text{m}^2$, $a = 0.25 \, \text{m}$, $\quad b = 0.28 \, \text{m}$,
$b_1 = 0.18 \, \text{m}$, $\quad H_0 = 0.225 \, \text{m}$, $\quad k_x = 5.957 \cdot 10^4 \, \text{N/m}$,
$k_y = 2.383 \cdot 10^4 \, \text{N/m}$, $k_\vartheta = 41.443 \, \text{N} \cdot \text{m}$, $k = 24.038 \, \text{N} \cdot \text{m}$.

The shear, longitudinal and rotational stiffnesses of springs are calculated by the formulas [11] for a spring with a wire diameter $d = 0.011 \, \text{m}$, average diameter of a spring coil $D = 0.08 \, \text{m}$, active coils $i = 12$ and the above spring height H_0 ($E = 2 \cdot 10^5 \, \text{MPa}$, $G = 8 \cdot 10^4 \, \text{MPa}$). The torsion stiffness of the flexible shaft is obtained for a hollow shaft with external and internal diameters, respectively $D_d = 0.06 \, \text{m}$, $d_d = 0.048 \, \text{m}$ and length $l_d = 0.25 \, \text{m}$ ($G_d = 8 \, \text{MPa}$ – shear modulus of durite material). The bending stiffness for the mentioned above shaft was assumed to be zero ($k_r = 0$). Values of the damping coefficients were determined from the natural frequencies of the free oscillations of partial systems in assumption that the dimensionless damping coefficient $\eta = 0,2$. The following values were obtained:

$\beta_x = 3.447 \cdot 10^3 \, \text{kg/sec}$; $\quad\quad \beta_y = 2.264 \cdot 10^3 \, \text{kg/sec}$,

$\beta_\vartheta = 138.5 \, \text{kg} \cdot \text{m}^2 / \sec$, $\beta_\gamma = 0.238 \, \text{kg} \cdot \text{m}^2 / \sec$.

The constant resistance torque of the rotor for vibration device was assumed to be equal to 5% from the nominal torque M_n IM. If the induction motor 4A100L6У3 is used then $M_d = 1.107 \, \text{N} \cdot \text{m}$. The catalog parameters of such IM: $N_n = 2.2 \, \text{kW}$; $n_0 = 1000 \, \text{prm}$ (synchronous rotational frequency); $s_n = 0.051$; $\mu_m = 2.2$; $\mu_u = 1.2$. Inertia moment of the motor rotor $J_e = 0.015 \, \text{kg} \cdot \text{m}^2$.

The following initial conditions have been used:
$\psi(0) = \varphi(0) = \pi/2$, $\quad\quad x(0) = y(0) = \vartheta(0) = 0$,
$M_D(0) = M_s$, $\dot\psi(0) = \dot\varphi(0) = 0$,
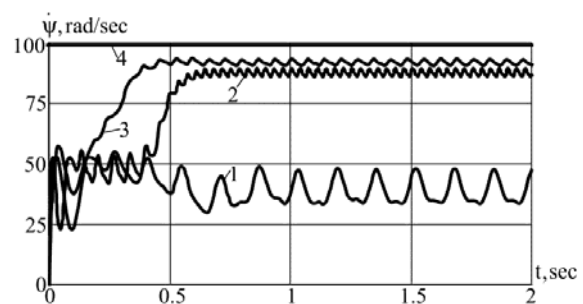$\dot x(0) = \dot y(0) = \dot\vartheta(0) = \dot M_D(0) = 0$ (see Fig. 1, 2).

Fig.3. Curves of the angular speed of the motor shaft depending on time at the moment of device starting: 1 – $N_n = 2.2 \, \text{kW}$, $a = 0.25 \, \text{m}$; 2 – $N_n = 2.2 \, \text{kW}$, $a = 0.245 \, \text{m}$; 3 – $N_n = 3 \, \text{kW}$, $a = 0.25 \, \text{m}$; 4 – ω_n

In Fig. 3 curves of the angular speed of the motor shaft depending on time are presented at the moment of device starting. For such parameter values $b = 0.35 \, \text{m}$, $b_1 = 0.25 \, \text{m}$, for the mentioned above motor starting is not possible – the angular speed of the shaft (curve 1) is less then 50% from nominal (line 4). The reason is that the natural frequency of rotational vibrations for the working

chamber has a relatively high value ($32.79\,\text{rad/sec}$). Therefore, the motor power is consumed mainly not for acceleration, but for intensive forced oscillations, which leads to its "speed hangup" [12, 17, 18]. Device starting with mentioned above parameters is possible (curve 3), if the following motor will be used 4A112MA6Y3 ($N_n = 3\,\text{kW}$). It, however, can be realized with the help of the original engine (curve 2), if the parameter value a will be reduced, characterizing the distance between springs. In this case, the natural frequency of the chamber rotational vibrations reduces due to a reducing of the corresponding equivalent stiffness. The maximum value of the mentioned above parameter, at which the starting process is still possible $a = 0.245\,\text{m}$.

From a technological point of view, the most important design elements of the mechanism are the eccentric shaft and unbalances. The mass magnitude, the unbalance shape, the eccentricity value of the rotor depends not only from motion state of the working chamber, but also on the possibility of the device coming into operational modes. Some calculations results of transient modes with different parameters values are given below. Most of them give a visual geometric interpretation, which is important for the parameters rational choice.
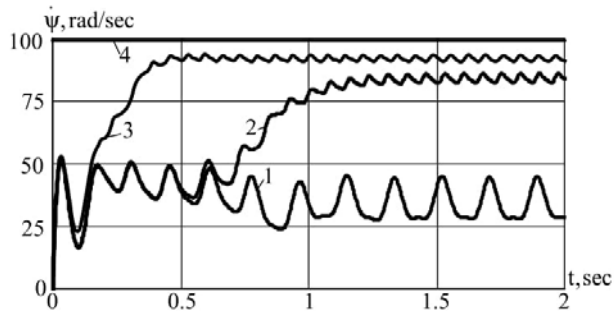

Fig. 4. Curves of the angular speed of the motor shaft depending on time at the moment of device starting: 1 – $m_d = 10.46\,\text{kg}$; 2 – $m_d = 10.42\,\text{kg}$; 3 – $m_d = 7.69\,\text{kg}$; 4 – ω_n
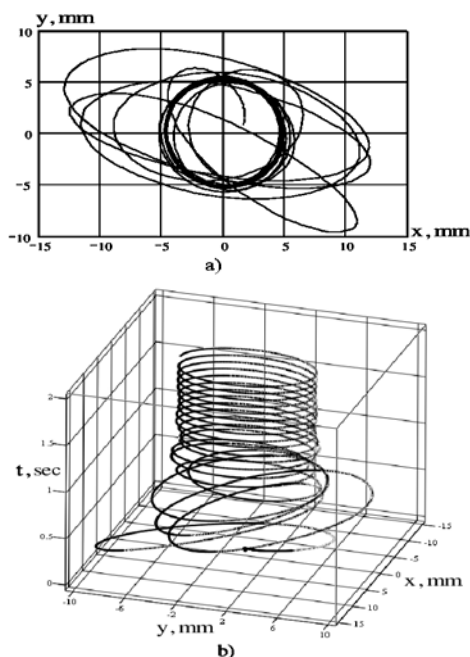

Fig. 5. Motion trajectory of the mass centre of the working chamber: a) – in plane; b) – in space

In Fig. 4 curves of the angular speed of the motor shaft depending on time at the moment of device starting are

shown: 4 – nominal; 3 – for the specified eccentricity values and the unbalances mass (see above); 2 – for limit values of the unbalances mass $m_d = 10.42\,\text{kg}$, at which the starting process can be realized; 1 – for values of the unbalances mass $m_d = 10.46\,\text{kg}$, more than limiting value. In last case the starting process can't be done – angular speed of the shaft is less than 50% from nominal value.

The Sommerfeld effect take a place - the motor power is consumed mainly not for acceleration, but for supporting of intense forced oscillations, which leads to its "hangup speed" [12, 19, 20, 22, 23]. Motion nature of the mass center of the working chamber at the device starting with limit unbalances is shown in Fig. 5: a) – coordinates variation in a plane; b) – three-dimensional graph (allow analyze additionally oscillations changing in time). The curve along which the mass center moves at steady mode (setting time approximately 1.5 sec) is close to a circle of radius 5 mm.
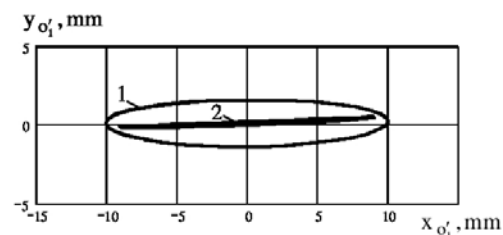

Fig. 6. Motion trajectory of the rotor axis with the eccentricity: 1 – $e = 2.5\,\text{mm}$; 2 – $e = 4.1\,\text{mm}$
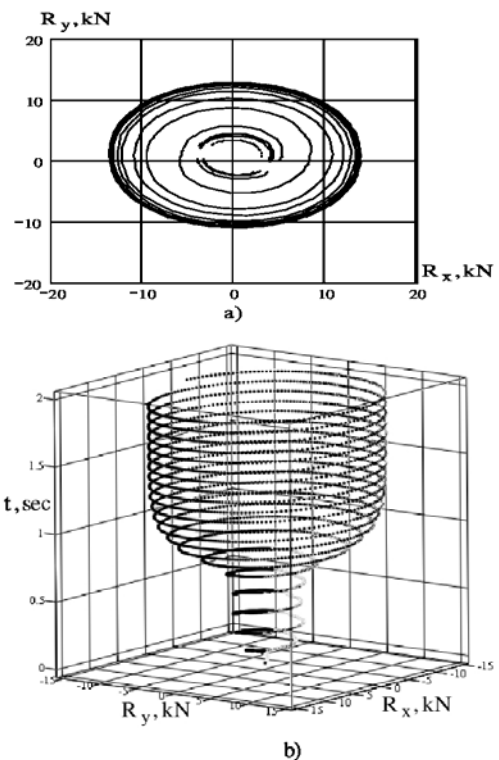

Fig. 7. Reaction projections of the rotor bearing on the fixed axis: a) – in plane; b) – in space

Analogous calculations of the rotor axis motions have shown that oscillations swings of the axis in the horizontal direction exceed the swings in the vertical direction. A rational choice of the rotor eccentricity allows significantly reduce axis oscillations at steady-state operational modes of the device (realization of the self-centering effect). In this case, dynamic loads on the flexible shaft and motor

bearings are reduced. In Fig.6 a motion graph of the rotor axis is shown when the eccentricity $e = 4.1mm$. The increase in eccentricity allowed practically removes vertical oscillations of the axis. For a rational choice of rotor bearings it is needed to know information about a load in them.

In Fig. 7 curves of changing the bearing reaction in time and space are shown. In accordance to the theorem of mass centre motion, projections of this reaction on the coordinate axes for a single bearing have the following form:

$$R_x = mx_m/2, \ R_y = (my_m + mg)/2,$$

and the module $R = \sqrt{R_x^2 + R_y^2}$, where x_m, y_m − mass centre coordinates of the rotor, for which take a place formulas (follow from the formulas for the coordinates transformation in plane motion; see Fig. 2):

$$\begin{cases} x_m = x_{C_1} = x + (e+r)cos\,\varphi \cdot cos\,\vartheta - (e+r)sin\,\varphi \cdot sin\,\vartheta + b\,sin\,\vartheta, \\ y_m = y_{C_1} = y + (e+r)cos\,\varphi \cdot sin\,\vartheta + (e+r)sin\,\varphi \cdot cos\,\vartheta - b\,cos\,\vartheta. \end{cases}$$

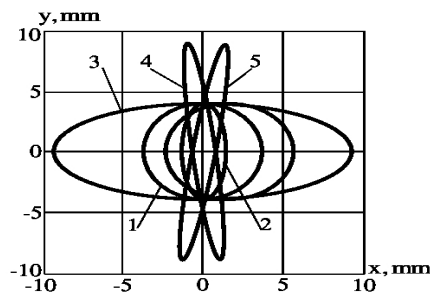The reaction maximum value at steady-state mode is close to 13 kN.

Fig. 8. Motion laws of working chamber points: 1 – mass centre of the chamber; 2 – point on the chamber axis; 3 – the lower point of vertical diameter; 4, 5 – left and right points of horizontal diameter, respectively

In Fig. 9 the dependence of a pressure force at foundation at the device starting is presented by following formula: $P = 2k_y(\Delta_1 + \Delta_2)$.
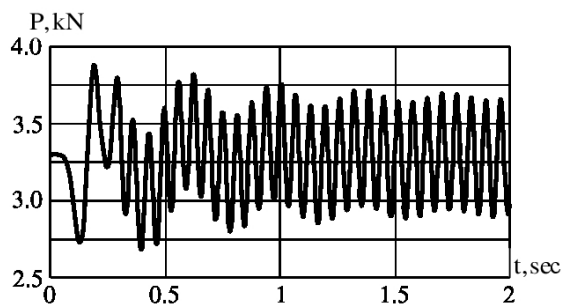
Fig. 9. Foundation pressure at device starting depending on time

In Fig. 8 the motion law of the characteristic points in the working chamber at steady-state mode is shown: 1 – mass centre of the chamber; 2 – point on the chamber axis; 3 – the lower point of vertical diameter; 4 and 5 – left and right points of horizontal diameter, respectively (see Fig.1, 2).

The curves equation after the differential equations integrations, is obtained by using the coordinate transformation formulas $x_i = x + x_i' cos\,\vartheta - y_i' sin\,\vartheta$, $y_i = y + x_i' sin\,\vartheta + y_i' cos\,\vartheta$, $(i = \overline{1,5})$, for comparison convenience the graphs are shown without taking into account axis shifts. It can be seen in figure that the

rotational oscillations can significantly affected on the points motion of the working chamber [21].

Conclusions

1. The complex mathematical model of vibration device on elastic supports with the eccentric unbalanced rotor and induction electric drive (Its working chamber does a plane motion) has been developed.
2. Differential equations of dynamic processes for the device mechanical part have been created.
3. The dynamic feature of the induction motor for adequately descriptions of device starting and a load oscillating character at steady-state operational modes of the device is chosen.
4. The converting method for consistent system of differential equations to a convenient form for numerical integration is proposed.
5 A visual method for geometric interpretation of the dynamic processes development at the device starting is given.
6. Calculations of the device with a help of developed model have been done:
- the motor and some parameters, which provide its starting, are chosen;
- the effect of unbalance parameters at device starting have been researched;
- oscillations parameters of mass centre of the working chamber and the rotor axis have been calculated;
- it is established that a rational choice of eccentricity allows to reduce the rotor vibrations (self-centering effect);
- motions of characteristic points of the working chamber at steady-state mode have been calculated;
- pressure forces on the foundation at device starting have been calculated.

Authors: Dr. Techn. Sc., Prof., Vladimir M. Shatokhin, Head of the Department of Theoretical Mechanics, Kharkiv National University of Civil Engineering and Architecture, 40 Sumska Str., Kharkiv, 61002, Ukraine, E-mail: shatokhinvlm@gmail.com; PhD. Techn. Sc., Ass. Prof., Vladimir M. Sobol, Department of Theoretical Mechanics, Kharkiv National University of Civil Engineering and Architecture, 40 Sumska Str., Kharkiv, 61002, Ukraine, E-mail: sobol_vn@ukr.net; Prof. Waldemar Wójcik, Lublin University of Technology, Institute of Electronics and Information Technology, Nadbystrzycka 38A, 20-618 Lublin, Poland, e-mail: waldemar.wojcik@pollub.pl; M.Sc. Gali Duskazaev, Kazakh Academy of Transport & Communication, email: dgali_94@mail.ru; M.Sc. Daniyar Jarykbassov, Kazakh Academy of Transport & Communication, email: danik.004@mail.ru

REFERENCES
[1] Shatokhin, V.M., About the identification of parameters of unbalanced oscillating devices with eccentric rotor and asynchronous drive, Vibrations in technique and technology, 3 (83) (2017), 41-50.
[2] Sylyvonyuk, A.V., Yaroshevich, A.V., About some features of dynamic acceleration of vibration machines with self-synchronisation inertion vibroexciters, Proceedings of XLI International Summer School–Conference APM 2013, (2013), 662-670.
[3] Mudrik, I., Measurement of dynamic properties of machine aggregate with variable parameters and asynchronous motor, J. Theor. and Appl. Mech., 23 (1) (1992), 40–41.
[4] Niselovskaya, E.V., Panovko, G.Ya., Shokhin, A.E., Oscillations of the mechanical system, excited by unbalanced rotor of induction motor. Journal of Machinery Manufacture and Reliability, 42 (6) (2013), 457–462.
[5] Shokhin, A.E., Nikiforov, A.E., On the Rational Dynamic Modes of Vibrating Machines with an Unbalanced Vibration Exciter of Limited Power. Journal of Machinery Manufacture and Reliability, 46 (5) (2017), 426–433.

[6] Tenhunen, A., Benedetti, T., Holopainen, T.P., Arkkio, A., Electromagnetic forces in cage induction motors with rotor eccentricity. Reprinted from Proceedings of IEMDC'03, Vol. 3. Madison, WI, USA, 1-4 June 2003, 3 (2003), 1616-1622.

[7] Karmakar, S., Chattopadhyay, S., Mitra, M., Sengupta, S., Induction Motor Fault Diagnosis. Approach through Current Signature Analysis, XXV (2016), 161.

[8] Aboul-Seoud, T., Jatskevich, J., Dynamic modeling of induction motor loads for transient voltage stability studies. 2008 IEEE Canada Ellectric Power Conference, (2008), 1-5.

[9] Yamna Hammou, Imene Kebabati, Abdellah Mansouri, New Algorithms of control and observation of the induction motor based on the sliding-mode theory, Electric power components and systems, 43 (2015), 520-532.

[10] Maxfield, B., Essential Mathcad for engineering, science, and math, Elsevier Science, (2009), 496.

[11] Vibrations in technique: In 6 volumes, ed. Dimmentberg, F.M. and Kolesnikova, K.S., Mechanical Engineering: Vol.3. Oscillations of machines, designs and their elements, (1980), 544.

[12] Karthikeyan, M., Alfa Bisoi, Samantaray, A.K., Bhattacharyya, R., Sommerfeld effect characterization in rotors with nonideal drive from ideal drive response and power balance, Mechanism and Machine Theory, 91 (2015), 269-288.

[13] Vasilevskyi, O.M. Metrological characteristics of the torque measurement of electric motors, International Journal of Metrology and Quality Engineering, 8, art. no. 7, (2017). DOI: 10.1051/ijmqe/2017005

[14] Vasilevskyi, O.M., Kulakov, P.I., Ovchynnykov, K.V., Didych, V.M. Evaluation of dynamic measurement uncertainty in the time domain in the application to high speed rotating machinery, International Journal of Metrology and Quality Engineering, 8, art. no. 25, (2017). DOI: 10.1051/ijmqe/2017019

[15] Vasilevskyi, O.M. Methods of determining the recalibration interval measurement tools based on the concept of uncertainty, Technical Electrodynamics, 2014 (6), 81-88.

[16] Vedmitskyi, Y.G., Kukharchuk, V.V., Hraniak, V.F. New non-system physical quantities for vibration monitoring of transient processes at hydropower facilities, integral vibratory accelerations // Przegląd Elektrotechniczny 93(3) (2017), 69-72.

[17] Kukharchuk, V.V., Kazyv, S.S., Bykovsky, S.A., Discrete wavelet transformation in spectral analysis of vibration processes at hydropower units. // Przegląd Elektrotechniczny 93(5) (2017), 65-68.

[18] Vasyl V. Kukharchuk, Valerii F. Hraniak, Yurii G. Vedmitskyi, Volodymyr V. Bogachuk, and etc. "Noncontact method of temperature measurement based on the phenomenon of the luminophor temperature decreasing", Proc. SPIE 10031, Photonics Applications in Astronomy, Communications, Industry, and High-Energy Physics Experiments 2016, 100312F (28 September 2016).

[19] Kukharchuk V.V., Bogachuk V.V., Hraniak V.F., Wójcik W., Suleimenov B., Karnakova G., "Method of magneto-elastic control of mechanic rigidity in assemblies of hydropower units", Proc. SPIE 10445, Photonics Applications in Astronomy, Communications, Industry, and High Energy Physics Experiments 2017, 104456A (7 August 2017).

[20] Azarov O. D., Dudnyk O.V., Kaduk O.V., Smolarz A., Burlibay A., "Method of correcting of the tracking ADC with weight redundancy conversion characteristic", Proc. SPIE 9816, Optical Fibers and Their Applications 2015, 98161V (17 December 2015).

[21] Osadchuk V.S., Osadchuk A.V. The magneticreactive effect in transistors for construction transducers of magnetic field // Electronics and Electrical Engineering. – Kaunas: Technologija, 109 (2011), 119-122.

[22] Korolova O., Cubillo J.T., Ponick B., Modelowanie stanów przejściowych maszyn prądu przemiennego z uwzględnieniem efektów drugiego rzędu, Informatyka Automatyka i Pomiary w Gospodarce i Ochronie Środowiska IAPGOŚ 8(2) (2018): 4-8.

[23] Listwan J., Direct torque control of multi-phase induction motor with fuzzy logic speed controller, Informatyka Automatyka i Pomiary w Gospodarce i Ochronie Środowiska IAPGOŚ 7(4) (2017), 38-43.